

Contactless 3D Fingerprint Identification Without 3D Reconstruction

Qian Zheng^{1,2}, Ajay Kumar¹, Gang Pan²

¹Department of Computing, The Hong Kong Polytechnic University, Kowloon, Hong Kong

²Department of Computer Science and Technology, Zhejiang University, Hangzhou, Zhejiang, China

Abstract

Recovery of 3D fingerprint data using photometric stereo generates 3D surface normal and albedo which forms rich 3D fingerprint surface information. These surface normal's are further subjected to the reconstruction process, which integrates the surface normal to generate depth data. Since the source of depth information is essentially the surface normal, it is prudent to examine if this source information can itself be used for 3D fingerprint identification. In addition to avoiding the errors introduced by well-known integrability problem, such an approach can also enable significantly faster identification as the 3D reconstruction is the most computationally complex operation before the template matching. This paper investigates such an approach for 3D fingerprint identification using recovered surface normal and albedo information. We use publicly available 3D fingerprint database from 240 clients for the performance evaluation. The experimental results presented in this paper are highly promising, validates our approach, and indicate promises from matching contactless 3D fingerprints without the 3D surface reconstruction.

Keywords— *Biometrics, 3D Fingerprint Identification, 3D Fingerprint Reconstruction, Contactless Fingerprint Matching*

1. Introduction

Automated fingerprint identification has been widely employed by the law-enforcement and civilian applications around the world for several years [1], [13]. Availability of low-cost imaging sensors, high storage and processing capabilities have motivated researchers to explore full potential from fingerprint modality and therefore several promising attempts have been made in the literature to realize contactless 3D fingerprint identification. Imaging, identification, interoperability and analysis of 3D contactless fingerprints is an emerging area of research in biometrics with significant potential to alter the way fingerprint modality is employed today. This paper focuses on such an effort towards more efficient 3D fingerprint identification. We present some promising results from this preliminary work to achieve 3D fingerprint identification from the direct source 3D information or *without* employing complex 3D surface reconstruction.

1.1. Related Work

Acquisition and identification of 3D fingerprint images has attracted the attention of many researchers and there are several promising attempts [2]-[5], [15], [23] in this area. Acquisition of 3D fingerprint images using structured lighting approach requires an additional fixed projector that projects patterned structured lighting illuminations. This approach is employed in [14] and detailed in [2], [5]. The matching strategy from such imaging in [2] acquires ridge information from the ridge geometry, instead of the surface albedo, and generates 3D fingerprint match scores using the height of these ridges. Despite higher cost and bulk associated with structured lighting based approach, this approach can enable high speed imaging and dense surface reconstruction. There are other methods of 3D fingerprint imaging using the range sensing such as the stereo imaging [26] and laser scanning. Earlier attempts [3]-[4] to acquire 3D fingerprint images employed multiple cameras that provided enhanced coverage of fingerprint regions and multiple images from such cameras were mosaiced together [11] to generate larger templates than those possible with the help of single camera. Such efforts essentially match multiple 2D fingerprint images acquired from multiple but different 3D views and there is very little (surface shape) or nil depth information is extracted from such stereo vision systems. However, such imaging [23] captures more information (2D surface area) and therefore results in more accurate and robust fingerprint identification. Acquisition of 3D fingerprints using photometric stereo has been recently introduced, *e.g.* in [15] or [25]. Photometric stereo is highly suitable for the acquisition of high frequency details, such as the ridges on 3D fingerprints, and offers low-cost alternative for the imaging as it only requires single fixed camera. Recent availability of 3D fingerprint databases in public domain has also attracted further research on contactless 3D fingerprint identification.

1.2. Our Work

The objective of this work has been to investigate on the possibility of matching 3D fingerprints without the need to incorporate time-consuming reconstruction process. The motivation is to incorporate fundamental information from 3D surface normal vectors and investigate potential from

such information for more accurate 3D fingerprint identification. The key idea is to exclude computationally complex process for 3D reconstruction which also introduces errors in the reconstructed fingerprints. These errors are introduced as its difficult to find closed form solutions for the integration, *i.e.*, integrability problem [6]-[8], and mainly results from the discontinuities around ridge valley boundaries.

We investigate a new approach for 3D fingerprint identification that does not incorporate 3D surface reconstruction process. In order to judiciously use the surface normal and albedo information acquired under photometric stereo imaging, we incorporate a series of operations that enable reliable extraction of minutiae information from the component images. Our experimental results using the publicly available 3D fingerprint database illustrate superior results and validate the promises from the approach investigated in this paper.

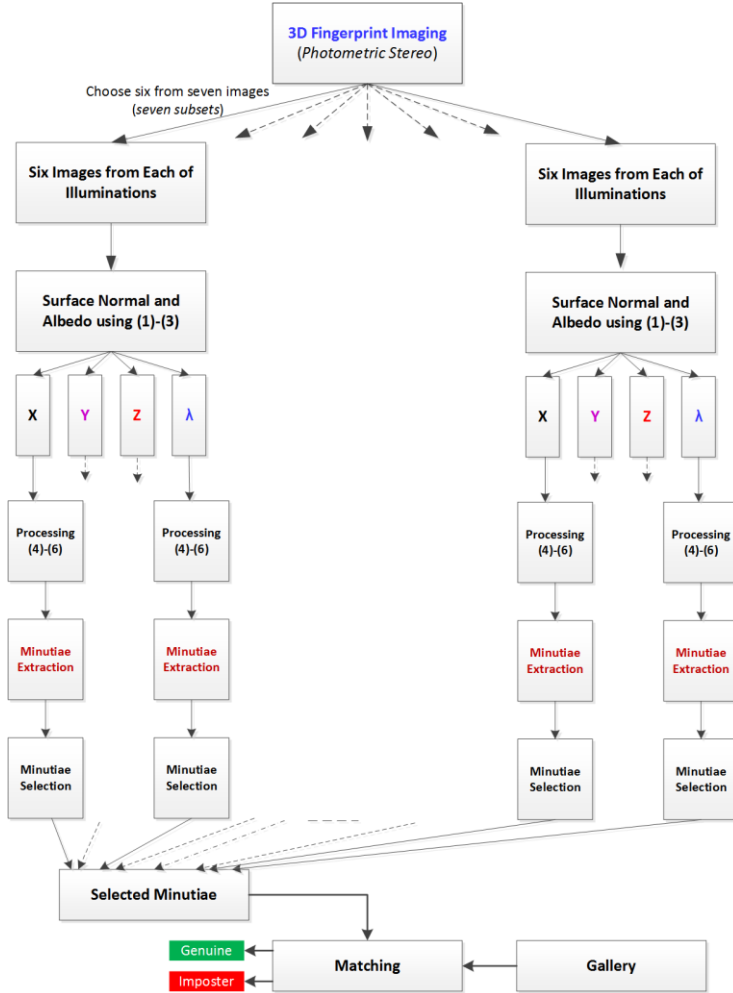


Figure 1: Block diagram for 3D fingerprint identification approach investigated in this paper.

2. 3D Fingerprint Acquisition using Photometric Stereo

Photometric stereo based imaging of 3D fingerprints requires single camera and can faithfully recover high frequency ridge information. This approach is largely based on the relationship between observed 2D image pixel intensity and the corresponding 3D surface normal information. Accurately reconstructing the 3D fingerprints surfaces (is highly desirable for accurately matching them), is challenging particularly under high intra-class variations that are mainly introduced due to pose changes that are common under such contactless imaging. One possibility to alleviate the errors introduced in the reconstruction of 3D fingerprints due to the well-known *integrability* problems is to exclude 3D reconstruction and use the fundamental source of 3D information, *i.e.*, surface normal, from the 3D fingerprint surface. Figure 1 illustrates the block diagram of such an approach investigated in this paper. We incorporate the recovered 3D surface normal and albedo information to more reliably recover the minutiae features for the 3D fingerprint identification. The key steps in this block diagram are described in the following sections.

2.1. Recovering 3D Fingerprint Surface Normals

Since the classical Lambertian based photometric stereo method can lose detail during the surface reconstruction, we divide the input images into several sets and use each set for the normal reconstruction. The more number of reconstructed normals are expected to increase 3D feature details as compared with those from one set of normal. The publicly available 3D fingerprint database has been acquired under seven different illuminations and therefore seven (noisy) images are available. One possibility is to group these seven images into seven subsets with each subset containing six images as shown in figure 1. Similar to as in [15] we also consider 3D finger surface as the Lambertian surface and is illuminated by m fixed LED light sources, *i.e.*, $\mathbf{L} = [l^1, l^2, \dots, l^m]^T$. Each of these LED sources (LED's) are calibrated from their fixed and known directions $l = [l_x, l_y, l_z]^T$. Let $\mathbf{n} = [n_x, n_y, n_z]^T$ represent unknown unit surface normal vectors on the 3D fingerprint surface. and \mathbf{I} be the observed pixel intensities in each of the m fingerprint images from the photometric imaging. The unknowns can be estimated from the least squared solution for the following equation:

$$\mathbf{b} = (\mathbf{L}^T \mathbf{L})^{-1} \mathbf{L}^T \mathbf{I} \quad (1)$$

where $\mathbf{L} \in \mathbf{R}^{6 \times 3}$ represents the illumination direction matrix, $\mathbf{I} \in \mathbf{R}^{3 \times 1}$ represents the intensity, and $\mathbf{b} \in \mathbf{R}^{3 \times 1}$ is a vector, the albedo λ and surface normal $\mathbf{n}(x, y, z)$ is computed by

$$\lambda = \text{norm}(\mathbf{b}), \quad (2)$$

$$\mathbf{n} = \mathbf{b} / \lambda \quad (3)$$

The surface normals and albedo recovered using (2)-(3) is

used as the source information and processed as detailed in the following sections.

2.2 Preprocessing 3D Surface Normals

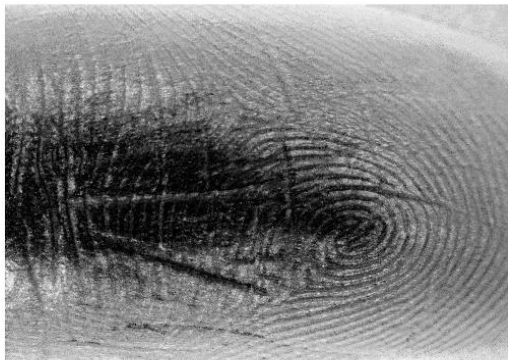
The surface normal reconstruction step enables us to recover seven surface normals for each of the client fingerprints as shown in Figure 1. Each of the 3D surface normals have four components; albedo, x -component, y -component, and z -component. Figure 2 illustrates The visualization of these components in gray level image for a client fingerprint in the database.



(a)



(b)



(c)



(d)

Figure 2: Visualization of (a) x -component, (b) y -component, (c) z -component and (d) albedo from a typical 3D fingerprint sample.

Then the preprocessing step is applied on these 28 (7×4) images (figure 1). The preprocessing method is inspired by the framework in [9], [12] to recover 3D feature descriptors from a *single* image. We therefore such spatial filters to encode the 3D information using the ordinal measurements. We use a spatial filter f to convolute with each of these 28 images and binarize the convoluted results. This preprocessing operation can be described as follows:

$$B = \tau(P * f) \quad (4)$$

where B is the binarized image or the preprocessed result (Figure 3), P is one of the 28 images, f is the spatial filter, and τ is the sign function which can be defined as follows:

$$\tau(\alpha) = \begin{cases} 0, & \alpha < 0 \\ 1, & \alpha \geq 0 \end{cases} \quad (5)$$

The spatial filter f [22] used in this work is defined as follows:

$$f_{i,j} = \begin{cases} 1, & |i| > |j| \\ -1, & |i| < |j| \\ 0, & |i| = |j| \end{cases} \quad (6)$$

In all our experiments, the size of spatial filter was fixed to set 13×13 .



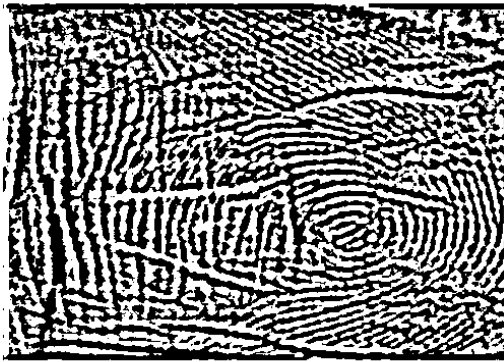
Figure 3: Sample 3D surface normal component image after the preprocessing operation.

2.3. Minutiae Extraction, Selection and Matching

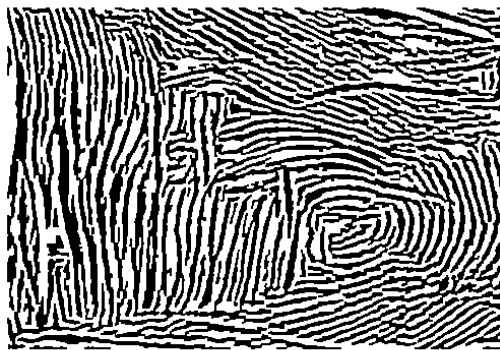
Each of the preprocessed images are used to extract minutiae features. There are several minutiae extraction algorithms and in this work we used BOZORTH3 implementation from NIST which is available in public domain [17]. This implementation also provides a quality score for each of the extracted minutiae. The binarized image after preprocessing generates a range of minutiae details. We therefore developed and incorporated an adaptive minutiae selection algorithm which is based on the minutiae quality. This algorithm is summarized as follow:

- We consider a minutiae *number* threshold T_2 (80) and select those minutiae whose *minutiae quality* is higher than T_1 (40);
- if the total minutiae *number* is smaller than T_2 , decrease T_1 and select the minutiae again;
- the selection process *ends* when $T_1 < 0$ or the selected minutiae *number* is larger than T_2 .

Above adaptive minutiae selection algorithm results in selection of higher quality minutiae as well as ensures that the number of selected minutiae are not too large.



(a)



(b)

Figure 4: Image samples for binary image (a) after preprocessing and (b) from using implementation in [17]. The match score from a client 3D fingerprint is generated from the list of selected minutiae. The best score among the

28×28 match pairs is returned as the matching score. The algorithm for the generation of final match score can be summarized as in the following.

```

Input: 28 selected minutiae sets  $N$  from probe
          28 selected minutiae sets  $M$  from gallery
set score:=0
for each minutiae set  $N_i$  from probe do
  for each minutiae set  $M_j$  from gallery do
    match  $N_i$  and  $M_j$  and get the matching score  $T$ 
    if score< $T$ 
      score:= $T$ 
    end if
  end for
end for
  
```

3. Experiments and Results

We used publicly available contactless 3D fingerprint database [21] for our experiments. This database also provides calibration information, *i.e.*, pixel positions, for the computations of the surface normal vectors. This database has been acquired from 240 different clients and each of the clients has provided 6 3D fingerprint images. The size of each of the seven region of interest fingerprint image from the photometric imaging is 350×700 pixels. The size of 3D surface normal images $3 \times 350 \times 700$. The average number of minutiae recovered from the preprocessed images was 62.204.

We performed matching experiments using all of the 240 client's 3D fingerprint images. Six 3D fingerprint images from each of the 240 clients generated 3600 (240×15)

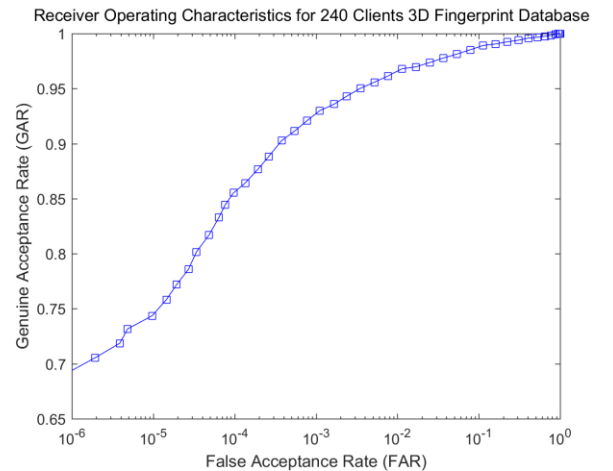


Figure 5: Receiver operating characteristics from the 3D fingerprint verification experiments.

genuine match scores and 2064960 ($240 \times 6 \times 6 \times 239$) impostor match scores. The receiver operating

characteristics using these match scores is shown in Figure 5. The equal error rate (EER) from this experiment is 2.49%.

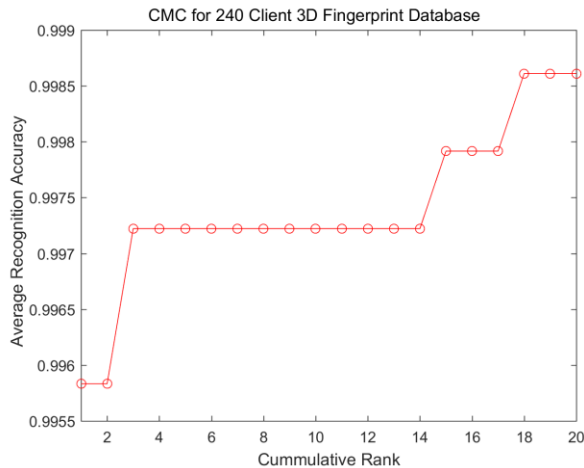


Figure 6: Cumulative match characteristics from the recognition experiments.

We also performed experiments to ascertain the performance for the 3D fingerprint recognition. The cumulative match characteristics from the recognition experiments is shown in Figure 6. It can be observed from this figure that the rank-one recognition accuracy is 99.1%. It may be noted that the rank-one accuracy in [15] by using 3D minutiae matching approach, by using same 3D fingerprint database and same matching protocols, is 94.75% while the equal error rate is 2.73%. Therefore, the achieved experimental results are highly encouraging and indicates promises from the proposed approach for the 3D fingerprint identification.

Table 1: Comparative Performance for 3D Fingerprints Matching.

Method	EER	Rank-One Accuracy
This Paper	2.49%	99.1%
3D Minutiae Matching [15]	2.73%	94.75%

3.1 Discussion

Although our approach for the 3D fingerprint identification excludes the 3D surface reconstruction, additional complexity is introduced due to seven pairs of surface normals generated in our framework. However, it should be noted that complexity for the computations of surface normal vectors (also for minutiae extraction/selection) is relatively much smaller as it only requires pixel *multiplication* since the term $(\mathbf{L}^T \mathbf{L})^{-1} \mathbf{L}^T$ is computed offline and stored for the multiplications during the online 3D fingerprint identification.

The key objective of the work detailed in this paper has been to comparatively ascertain if the sensed or *source* 3D information during 3D fingerprint *imaging* process can itself be utilized to more accurately match 3D fingerprints. Therefore the comparison with 3D fingerprint minutiae matching approach, which represents 3D information and offers better performance than 3D surface curvature based features in [15], is justified. It should also be noted that experiments in [15] provides comparison with 3D fingerprint matching with *multiple noisy* 2D fingerprints. Therefore it is not reasonable to infer that 2D fingerprint matching illustrates superior matching accuracy over 3D fingerprint matching from the results presented in [15].

4. Conclusions and Further Work

This paper has investigated a new approach for the contactless 3D fingerprint identification. The key motivation for this investigation has been to *alleviate* the 3D reconstruction step, which is the most complex step and also known to introduce errors due to the well-known integrability problem. Therefore, we investigated a new framework (Figure 1) to match 3D fingerprints using the surface normal vectors and albedo information, which appropriately represents source 3D information. This framework incorporated multiple pieces of sensed 3D information and preprocessed the component features to recover the 3D descriptors introduced in [12]. The experimental results presented in this paper using publicly available 3D fingerprints database indicates promises from this approach. These results indicate the possibility that the source information acquired to reconstruct the 3D fingerprint model can itself be used to achieve superior matching accuracy.

Our motivation has been to ascertain the accuracy from a new approach for the 3D fingerprint identification and we achieved outperforming or very encouraging results. However, the investigation detailed in this paper should only be considered preliminary as there are several limitations. The computational benefits from this approach are only qualitatively analyzed and exact quantitative numbers to validate the computational benefits can be more convincing and desirable. The performance from binarized features generated in (6) can be improved by considering their consistency or fragility, similar to as in [24], and needs to be explored in the further extension of this work. Similar to as in [15], our work assumes that the finger skin surface can be modeled as the Lambertian surfaces which however may not be true. The real image formation from contactless photometric stereo imaging is much more complex. Therefore, further work should consider practical 3D image formation model, incorporate intra-class variations due to perspective changes and the finger motion, to develop more accurate for contactless 3D fingerprint identification.

Acknowledgment

This work is supported by General Research Fund from Research Grant Council of Hong Kong, project number PolyU 516913, and project number PolyU 152129/15E.

References

- [1] G. Parziale and Y. Chen, "Advanced technologies for touchless fingerprint recognition," *Handbook of Remote Biometrics*, M. Tistarelli, Stan. Z. Li, R. Chellappa, (Eds.), pp. 83-109, Springer-Verlag London, 2009.
- [2] Y. Wang, L. G. Hassebrook, D. L. Lau, "Data acquisition and processing of 3-D fingerprints," *IEEE Trans. Info. Forensics & Security*, pp. 750-760, Dec. 2010.
- [3] G. Parziale, E. Diaz-Santana and R. Hauke, "The surround imager: A multi-camera touchless device to acquire 3d rolled-equivalent fingerprints," *Proc. ICB 2006*, LNCS, vol. 3832, Jan 2006.
- [4] R. D. Labati, V. Piuri, F. Scotti. *Touchless Fingerprint Biometrics*. CRC Press, 2015.
- [5] F. Chen, "3D fingerprint and palm print data model and capture devices using multi structured lights and cameras," *US Patent No. 7609865*, Oct. 2009.
- [6] T. Simchony, R. Chellappa, and M. Shao, "Direct analytical methods for solving poisson equations in computer vision problems," *IEEE Trans. Pattern Analysis & Machine Intelligence.*, pp. 435-436, Dec. 1990.
- [7] A. Agrawal, R. Raskar and R. Chellappa, "What is the range of surface reconstructions from a gradient field?," *Proc. 9th European Conference on Computer Vision*, Graz, Austria, May 2006.
- [8] T. Frankot and R. Chellappa, "A method for enforcing integrability in shape from," *Proc. Int'l Conf. Computer Vision*, ICCV, 1987.
- [9] A. Kumar and Q. Zheng, "A method and device for contactless biometrics identification," *U. S. Patent No. 14798573*, July 2017.
- [10] L. Hong, Y. Wan and A. K. Jain, "Fingerprint image enhancement: algorithms and performance evaluation," *IEEE Trans. Pattern Analysis & Machine Intelligence.*, vol. 20, pp. 777-789, Aug. 1998.
- [11] H. Choi, K. Choi and J. Kim, "Mosaicing touchless and mirror-reflected fingerprint images," *IEEE Trans. Info. Forensics & Security*, no. 5, pp. 52-61, Mar. 2010.
- [12] Q. Zheng, A. Kumar, G. Pang, "A 3D feature descriptor recovered from a single 2D palmprint image," *IEEE Trans. Pattern Analysis & Machine Intelligence.*, vol. 38, pp. 1272-1279, June 2016.
- [13] *Handbook of Fingerprint Recognition*, D. Maltoni, D. Maio, A. K. Jain, and S. Prabhakar, Springer Verlag, Second Ed., 2009.
- [14] Flashscan3d, <http://www.flashscan3d.com>, accessed Dec. 2016
- [15] A. Kumar and C. Kwong, "Towards contactless, low-cost and accurate 3d fingerprint identification," *IEEE Trans. Pattern Analysis & Machine Intelligence.*, vol. 37, pp. 681-696, Mar. 2015.
- [16] T.-Y. Jea and V. Govindaraju, "A minutiae-based partial fingerprint recognition system," *Pattern Recognition*, vol. 38, no. 10, pp. 1672-1684, 2005.
- [17] NIST Biometric Image Software, NBIS Release 5.0.0, <http://www.nist.gov/itl/iad/ig/nbis.cfm>, 2016.
- [18] Y. Chen, G. Parziale, E. Diaz-Santana, and A. K. Jain, "3D Touchless fingerprints: Compatibility with legacy rolled images," *Proc. BCC 2006*, Tampa, 2006.
- [19] S. Pankanti, S. Prabhakar, and A. K. Jain, "On the individuality of fingerprints," *IEEE Trans. Pattern Anal. Mach. Intell.* 24, 1010-1025 (2002).
- [20] R. Cappelli, D. Maio, D. Maltoni, J. L. Wayman, and A. K. Jain, "Performance evaluation of fingerprint verification systems," *IEEE Trans. Pattern Analysis & Machine Intelligence.*, vol. 28, pp. 3-18, 2006.
- [21] The Hong Kong Polytechnic University 3D Fingerprint Images Database, 2016. <http://www.comp.polyu.edu.hk/~csajaykr/3Dfingerprint.htm>
- [22] A. Kumar and Z. Xu, "Personal identification using minor knuckle patterns from palm dorsal surface," *IEEE Trans. Info. Forensics and Security*, pp. 2338-2348, Oct. 2016.
- [23] C. Lee, S. Lee, and J. Kim, "A study of touchless fingerprint recognition system," in *Structural, Syntactic, and Statistical Pattern Recognition*. Springer, 2006, pp. 358-365.
- [24] C.-W. Tan and A. Kumar, "Accurate iris recognition at a distance using stabilized iris encoding and Zernike moments phase features," *IEEE Trans. Image Process.*, vol. 23, pp. 3962-3974, July. 2014.
- [25] A. Kumar and C. Kwong, "Towards contactless, low-cost and accurate 3d fingerprint identification," *Proc. CVPR 2013*, Jun. 2013.
- [26] R. D. Labati, A. Genovese, V. Piuri, F. Scotti, "Toward unconstrained fingerprint recognition: a fully-touchless 3-D system based on two views on the move," *IEEE Trans. Systems, Man, and Cybernetics: Systems*, pp. 202-219, Feb., 2016.